

DOE/ER/10390--1

Progress Report

INVESTIGATION OF DEEP LEVEL DEFECTS IN EPITAXIAL SEMICONDUCTING
ZINC SULPHO-SELENIDE

B. W. Wessels

Northwestern University
Evanston, Illinois 60201

March 1980

Report for the Period 6/15/79 - 6/14/80

MASTER

Prepared for the Department of Energy under
Contract No. DE-AS02-79-ER 10390

DISCLAIMER

This book was prepared as an account of work sponsored by an agency of the United States Government. Neither the United States Government nor any agency thereof, nor any of their employees, makes any warranty, express or implied, or assumes any legal liability or responsibility for the accuracy, completeness, or usefulness of any information, apparatus, product, or process disclosed, or represents that its use would not infringe privately owned rights. Reference herein to any specific commercial product, process, or service by trade name, trademark, manufacturer, or otherwise, does not necessarily constitute or imply its endorsement, recommendation, or favoring by the United States Government or any agency thereof. The views and opinions of authors expressed herein do not necessarily state or reflect those of the United States Government or any agency thereof.

NOTICE

This report was prepared as an account of work sponsored by the United States Government. Neither the United States nor the United States Energy Research and Development Administration, nor any of their employees, nor any of their contractors, subcontractors, or their employees, makes any warranty, express or implied, or assumes any legal liability or responsibility for the accuracy, completeness, or usefulness of any information, apparatus, product or process disclosed or represents that its use would not infringe privately owned rights.

DISTRIBUTION OF THIS DOCUMENT IS UNLIMITED

DISCLAIMER

This report was prepared as an account of work sponsored by an agency of the United States Government. Neither the United States Government nor any agency Thereof, nor any of their employees, makes any warranty, express or implied, or assumes any legal liability or responsibility for the accuracy, completeness, or usefulness of any information, apparatus, product, or process disclosed, or represents that its use would not infringe privately owned rights. Reference herein to any specific commercial product, process, or service by trade name, trademark, manufacturer, or otherwise does not necessarily constitute or imply its endorsement, recommendation, or favoring by the United States Government or any agency thereof. The views and opinions of authors expressed herein do not necessarily state or reflect those of the United States Government or any agency thereof.

DISCLAIMER

Portions of this document may be illegible in electronic image products. Images are produced from the best available original document.

ABSTRACT

In an effort to understand the defect structure of the ternary II-VI compound zinc sulpho-selenide, the binary compound zinc selenide was investigated. Thin single crystalline films of zinc selenide were heteroepitaxially grown on (100) GaAs. Epitaxial layers from 5 - 50 microns thick could be readily grown using a chemical vapor transport technique. The layers had an excellent morphology with few stacking faults and hillocks. Detailed epitaxial growth kinetics were examined as a function of temperature and reactant concentration. It was found that hydrogen flow rate, source and substrate temperature affect the growth rate of the epitaxial films.

Au - ZnSe Schottky barrier diodes and ZnSe - GaAs n-p heterojunctions were prepared from the epitaxial layers. Current-voltage characteristics were measured on both types of diodes. From capacitance-voltage measurements the residual doping density of the epitaxial layers were found to be of the order of 10^{14} - 10^{15} cm^{-3} . Finally, we have begun to measure the deep level spectrum of both the Schottky barrier diodes and the heterojunctions. Deep level transient spectroscopy appears to be well suited for determining trapping states in ZnSe provided the material has a low enough resistivity.

PROGRESS REPORT

II-VI compounds are of considerable interest for use in a number of electro-optic applications. However, in many cases their use is limited because of the difficulty in obtaining bipolar conductivity in these compounds. There are a number of phenomena that could account for the difficulty; they include compensation by unwanted impurities, low solubility of certain dopants, high ionization energies of acceptor and donor states, and self-compensation of deliberately added dopants. The research carried out over the period June 15, 1979 - March 15, 1980 examined the possible origins of compensation mechanisms in zinc sulpho-selenide, a material that has been recently been prepared in both n and p-type conducting states. Research was carried out in three main areas which included preparation of high purity epitaxial ZnSe, electrical characterization of the epitaxial material, and detection of deep level defects in ZnSe. The binary compound zinc selenide was investigated initially since this constitutes the major constituent of the ternary $ZnS_x Se_{1-x}$.

PREPARATION OF EPITAXIAL ZnSe

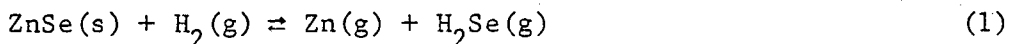
During this period, the technique for the epitaxial growth of ZnSe was developed. Thin single crystalline films of ZnSe with low defect densities were routinely grown heteroepitaxially on (100) oriented GaAs substrates, using open tube chemical vapor transport. The reactant system used was ZnSe - H₂ - H₂S. This particular system was chosen over the Zn - H₂Se - H₂ - HCl - H₂S system for simplicity as well as for other considera-

tions. For instance, chlorine, which is a constituent of the latter system, is a known n-type dopant in ZnSe and consequently would preclude the possibility of making uncompensated p-type material.

The deposition system used in this study consisted of a two-zone resistance heated furnace, and a high purity GE 214 quartz reaction tube. The reactant gases included electronic grade mixture of 15% H_2S in hydrogen and palladium diffused hydrogen as the carrier gas. Electronic grade ZnSe (GE or Eagle Picher) served as the source of ZnSe for chemical vapor transport. Before growth, ZnSe was baked in hydrogen for one hour at $1000^\circ C$ and subsequently remained in a hydrogen atmosphere at $200^\circ C$. It was found that baking of the source was a key factor in obtaining defect free ZnSe layers. Epitaxial layers were grown on gallium arsenide wafers, oriented 2° off the (100) plane towards the (110). Both n and p-type wafers were used. Before deposition the polished wafers were chemically etched in 3:1:1 H_2SO_4 : H_2O : H_2O_2 .

Typical growth conditions consisted of a ZnSe source temperature of $950^\circ - 1000^\circ C$ and a substrate temperature of $720^\circ - 820^\circ C$. A typical furnace profile used in the crystal experiments is shown in Fig. (1). For a source temperature of $1000^\circ C$, a substrate temperature of $750^\circ C$ and a H_2 flow rate of 500 cc/min. a growth rate of $0.3 \mu m/min$ was observed. During the period of June 15 - Feb. 15, a total of one hundred and seven crystal growth experiments were performed.

It was found that the growth rate, thin film thickness and epitaxial layer morphology were affected by a number of parameters including, source temperature, substrate temperature and hydrogen flow rate. The growth conditions were varied in order to understand the growth kinetics of the thin films. An understanding of the crystal growth kinetics is necessary in order to obtain films with the desired properties. As shown in Fig. (2) the ZnSe source weight loss rate was a function of temperature. From the Arrhenius plot, an activation energy of 32 kcal/mole was determined. This enthalpy corresponds to that observed for the reaction:



Thus increasing the source temperature significantly increases the flux under which the epitaxial ZnSe grows. Consequently, high temperatures are desired for optimal growth rates.

As shown in Fig. (3) a linear relationship between flow rate of H_2 and source depletion rate was observed for flow rates less than 0.6 liters/min. This is consistent with the source being in quasi-equilibrium with the gas stream. Under these conditions the weight loss per unit time is then given by

$$W = P_{\text{Zn}} V_o M(RT_o)^{-1} \quad (2)$$

for ZnSe, where P_{Zn} is the partial pressure of zinc, V_o is the flow rate at room temperature T_o and M is the molecular weight of zinc selenide.

For quasi-equilibrium conditions the layer growth rate G is given by

$$G = \Delta P_{\text{Zn}} V_o M(RT_o S_p)^{-1} \quad (3)$$

would be expected, where ΔP_{Zn} is the difference in the equilibrium partial

pressure between source and substrate, S the reactor cross sectional area; ρ is the density of ZnSe. According to Eq. 3, the growth rate is proportional to the flow rate. Fig. 4 shows that up to flow rates of .6 liters/min the growth rate is indeed proportional to flow rate.

Provided that there is a significant temperature difference between the source and the substrate Eq. 3 can be simplified to

$$G = W(S\rho)^{-1} \quad (4)$$

Eq. 4 indicates that the epitaxial growth rate G is proportional to the rate of source depletion W . As can be seen from Fig. 5 there is a strong correlation between growth rate and source depletion rate for flow rates lower than 0.6 l/min, suggesting that the quasi equilibrium model holds for transport of ZnSe to the substrate region of the CVD reactor.

Besides source temperature and flow rate, substrate temperature was found to influence the growth kinetics. An exponential decrease in growth rate was observed for decreasing substrate temperature, as shown in Fig. 6. From the Arrhenius plot of growth rate vs. $1/T$, an activation energy of 25 Kcal/mole was observed. Since the crystal growth rate appears to be an activated process, it is concluded from this study that adsorption plays the critical role in the growth kinetics of ZnSe.

Although different starting reactants were used, the experimental data in Fig. 6 obtained in this study are in excellent agreement with the ZnSe growth data reported by Yim and Stofko. In their system, the ZnSe was prepared using the HCl-hydride technique. This suggests that substrate temperature is one of the more important kinetic parameters in determining

growth rate and not necessarily starting reactants.

Eq. 4 only predicts the maximum growth rate that can be expected for the ZnSe epitaxial layers. Kinetic factors such as surface diffusion, desorption and adsorption can further limit the expected growth rate. This appears to be the case since the growth rate of the layer is an activated process. Thus the heteroepitaxy of ZnSe on GaAs by chemical vapor deposition can thought to be a three step process: (1) saturation of the ambient with Zn and H_2Se at the source, which occurs under quasi-equilibrium (2) transport of the Zn and H_2Se from the source to the substrate and (3) the adsorption and subsequent growth of the thin film which is limited by surface kinetics. The first and third processes appear to be the rate limiting steps in the growth of the thin films.

In addition to crystal growth kinetic experiments, the structure of the films was ascertained using scanning Auger microscopy, optical microscopy and scanning electron microscopy. With the scanning electron microscope using channeling techniques the epitaxial films were shown to be single crystalline. The film composition was determined using a scanning Auger microscope, and was shown to be ZnSe. Observation with an optical microscope of the thin films of ZnSe have shown that the films are essentially void of macrodefects such as stacking faults and growth hillocks. On the basis of morphological quality, the ZnSe epitaxial layers developed during this period seemed to be well suited for device studies.

ELECTRONIC PROPERTIES

Two types of junctions were examined in order to electrically characterize the thin films of single crystalline ZnSe. Schottky barriers were prepared by vacuum deposition of 5000°A of gold through a mask. In these studies the average diode area was 0.8mm^2 . Before deposition, the ZnSe layers were etched in HCl/HNO_3 . A thin layer of silver paint was applied to the gold dots in order to make wire contacts to the Schottky barriers. Ohmic contacts to the n^+ GaAs substrates were indium dots which were alloyed at 250°C in a hydrogen atmosphere. The n^+ GaAs served as an ohmic contact to the n-type ZnSe.

Typical current density-voltage characteristics of the Au-ZnSe Schottky barriers are given in Fig. 7. In the forward voltage direction the diodes could be expressed by the equation

$$J_F = J_0 \exp (-eV/AKT) \quad (5)$$

where A and J_0 are constants. For the diodes investigated A was found to vary between 2 and 5. Values of $A = 1$ are consistent with injection through a Schottky barrier. The increase in the A values is not understood at present but it may signal formation of a compound between the metal and the ZnSe. The extrapolated values for J_0 are given in Table 1. The relatively small magnitude of the extrapolated value of current density suggests that the Schottky barriers are of good quality. Reverse breakdown voltages of the Schottky barrier ranged from 3 - 15V. The high breakdown voltages indicate again that the junctions are of good quality. However, it also indicates that the residual doping density of the ZnSe epitaxial films is low.

In order to ascertain the doping density of the films capacitance-voltage measurements were performed on the Schottky barriers. Values of the capacitance

at zero bias ranged from 10 to 60 pF/mm². By plotting the variation $1/C^2$ vs V where C is the capacitance and V is the voltage the dopant density was obtained according to the equation

$$1/C^2 = \frac{2}{q E_s N_d} (V_{bi} + V) \quad (6)$$

where N_d is the doping density, E_s the relative dielectric constant and V_{bi} the Schottky barrier height. As can be seen from Fig. 8, relatively little variation in the capacitance as a function of voltage was observed for the diodes, which indicates the residual donor density was quite low. Fig. 9 shows a typical plot of the variation of $1/C^2$ vs V. The values of the donor density for several different layers are reported in Table 2. The donor densities of the as-grown layers varied between $1 \times 10^{14} \text{ cm}^{-3}$ and $1 \times 10^{15} \text{ cm}^{-3}$.

Current density-voltage characteristics were also measured on thin film ZnSe-GaAs n-p heterojunctions prepared as follows. The GaAs substrate was p-type having a carrier concentration of $2 \times 10^{17} \text{ cm}^{-3}$. The ZnSe epitaxial layers were 5-10 μm thick. After deposition of ZnSe on the GaAs substrates, the back-side was mechanically polished to remove the ZnSe layer and subsequently etched in a dilute solution of HCl/HNO₃. After scribing indium ohmic contacts were alloyed to the ZnSe layer as well as the GaAs substrate at 250°C.

Forward J-V characteristics were measured on the n-p heterojunctions. For the range of conditions investigated, the current voltage characteristics could be expressed by

$$J_f = J_o (\exp \frac{eV}{AKT} - 1) \quad (7)$$

In the case of heterodiodes the diode quality factor A should ideally vary

between 1 and 2. For the diodes fabricated by the CVD in this study A varied between 1.3 and 2.1. The extrapolated values of J_0 varied between 10^{-6} and 10^{-10} amps/cm² which is of the same order reported ZnSe-GaAs heterojunctions prepared by close-space vapor transport. The relatively low J_0 values indicate that the ZnSe/GaAs heterojunctions may be suitable for photovoltaic devices provided the conductivity of the ZnSe can be controlled.

Fig. 11 shows the capacitance-voltage characteristics of the n-p heterojunctions plotted in the form $1/C^2$ vs. V. From the C-V data the carrier concentration in the zinc selenide region of the heterojunction was obtained. For the different diodes investigated the measured dopant concentrated varied between 1×10^{14} and 2×10^{16} cm⁻³.

The built-in voltages obtained from C-V measurements were usually greater than 5 volts. This is considerably higher than the 1.3 V which would be expected using the Anderson heterojunction model for predicting built-in voltages. The variation is not understood at present and is the subject of further investigation.

It should be noted that the donor density measured for the ZnSe heterojunction is somewhat higher than that measured by Schottky barriers on the material. This suggests that some interdiffusion at the heterojunction is taking place, that is the ZnSe may be doped with Ga which comes from the substrate.

The measured residual donor densities appear to be quite high when compared to ZnSe prepared by other techniques such as close space vapor transport. Usually the as-grown material have reported resistivities of the order of 10^8 ohm-cm, which corresponds to a donor density of 2×10^8 cm^{-3} . This is some six to eight orders of magnitude less than what we observe. It should be noted that our values of carrier concentration are based solely on C-V measurements. Verification of these results by using Hall measurements is currently underway.

DEEP LEVEL TRANSIENT SPECTROSCOPY STUDIES

In work related to but not supported by this project, over the past year several II-VI compounds have been investigated with deep level transient spectroscopic techniques in order to ascertain its applicability to semiconducting systems other than silicon and III-V compounds. Systems investigated included the GaAs - CdS heterojunction structure and the Cu-CdS Schottky barrier junction. Detailed information on the trap distribution, energies and concentration was gained for these systems.

Preliminary investigations using DLTS have begun on the ZnSe semiconducting system. DLTS measurements have been performed on both the Schottky barriers and heterojunction structures. This represents to our knowledge the first reported use of DLTS on wide band gap semiconductors and suggests the wide applicability of this technique in defect investigations in semiconducting systems.

The DLTS spectrum for a characteristic ZnSe/GaAs heterojunction is given in Fig. 12. Since the doping density of the p-type GaAs substrates was 2.5×10^{17}

cm^{-3} , the traps observed were located in the ZnSe side of the depletion layer where the carrier concentration is of the order of 10^{15} cm^{-3} . The observed spectrum with its characteristic peaks is indicative of discrete deep level states.

Fig. 13 shows the measured thermal emission rates as a function of reciprocal temperature for the deep trapping levels observed in the heterojunctions. From the temperature dependence of the emission rate, the binding energies and approximate values of the capture cross-section were obtained using the detailed balance equation given by

$$e_n = \tau^{-1} = N_c \sigma_\infty \langle v \rangle \exp(-\Delta E_t / kT) \quad (8)$$

where σ_∞ is the capture cross section, $\langle v \rangle$ is the thermal velocity, ΔE_t is the trap energy and N_c is the effective density of states in the conduction band. In Eq. (8) the capture cross section is assumed to be temperature independent. In the determination of the trap binding energies and cross-sections, only the T^2 dependence of $N_c \langle v \rangle$ was taken into account. Values for the capture cross-sections for the different traps are reported in Table (3). As reported in Table (3), a total of four different traps were observed in the ZnSe/GaAs heterojunctions. It should be noted that these traps were not systematically observed in every sample.

We observed that in heterojunctions with donor concentrations of less than 10^{15} cm^{-3} no traps were observed. This probably occurred as a result of the inability of the present DLTS setup to modulate the space charge width of the heterojunctions constructed from materials of greater than $100 \Omega\text{-cm}$ resistance.

As for the Schottky barrier DLTS studies, preliminary data was obtained. Fig. 14 shows the DLTS spectrum for Au-ZnSe diodes. For this diode a single trap with an activation energy of 0.71 eV below the conduction band with a concentration of $1 \times 10^{13} \text{ cm}^{-3}$ was observed. The identity of the trap is not yet known. It should be noted that most of the Schottky barrier samples had carrier concentrations of less than 10^{15} cm^{-3} . Consequently most of the time traps were not observed because of the high resistance of the samples. Subsequent studies are aimed at looking a deliberately doped ZnSe with resistivities of less than 100 $\Omega\text{-cm}$.

WORK PROJECTED BETWEEN 15 MARCH and 15 JUNE 1980

1. We plan to change the stoichiometry of the ZnSe films by growing under zinc rich conditions. In addition, we plan to dope the ZnSe films with indium and aluminum.
2. Initial preparation of the ternary zinc sulpho-selenide will begin. The composition will be determined using scanning Auger spectroscopy as well as x-ray microprobe analysis.
3. Hall measurements on ZnSe epitaxially grown on chromium doped GaAs will begin.
4. Deep level spectroscopy measurements on deliberately doped ZnSe will be started.

EFFORT DEVOTED TO THIS PROJECT

During the academic year the principal investigator has spent 10% of his time on this project; summer effort was 100% of the time for one and one-half months. The 10% time effort will be continued until 15 June 1980. Two full time graduate research assistants, Mr. Paul Besomi and Mr. Wallace Leigh, have been associated with this project. P. Besomi has been with the project since June 15, 1979 and W. Leigh since Sept 15, 1979. In addition, two part time undergraduate technicians have been associated with the project.

PUBLICATIONS

None - new start.

PRESENTATIONS

"Growth and Characterization of Heteroepitaxial Zinc Selenide" to be presented at Electronic Materials Meeting of the A.I.M.E., Cornell University, June 1980.

FIGURE CAPTIONS

Fig. 1 Temperature profile used for chemical transport in the ZnSe/H₂ open tube system.

Fig. 2 Source depletion rate as a function of temperature. The hydrogen flow rate over the source was 0.5 liters/min.

Fig. 3 Source depletion rate as a function of H₂ flow rate, for a source temperature of 1000°C.

Fig. 4 Growth rate versus H₂ flow rate for a source temperature of 1000°C.

Fig. 5 Growth rates versus source depletion rate for a source temperature of 1000°C and a substrate temperature of 750°C.

Fig. 6 Epitaxial growth rate as a function of temperature. The total hydrogen flow rate was 750 cc/min. and the source temperature was 1000°C.

Fig. 7 Current density - voltage characteristic of Au-ZnSe Schottky barrier diode. The diode area is $8 \times 10^{-3} \text{ cm}^2$.

Fig. 8 Capacitance versus voltage for Au-ZnSe Schottky barrier diodes curve (1) $N_D - N_A = 1.2 \times 10^{15} \text{ cm}^{-3}$, $V_{bi} = 3.5 \text{ V}$.

Fig. 9 The variation of $1/C^2$ with voltage for a Au-ZnSe diode.

Fig. 10 Current density-voltage characteristic of a ZnSe-GaAs heterojunction grown by chemical vapor transport. The diode area is 10^{-2} cm^2 .

Fig. 11 Capacitance-voltage characteristic of a ZnSe-GaAs heterojunction.

Fig. 12 Observed DLTS spectrum for a ZnSe-GaAs heterojunction. The rate window is $4.62 \times 10^3 \text{ sec}^{-1}$.

Fig. 13 Arrhenius plot of emission rate constants for traps observed in ZnSe-GaAs heterojunctions.

Fig. 14 Observed DLTS spectrum for a Au-ZnSe Schottky barrier junction. The rate window is $4.62 \times 10^3 \text{ sec}^{-1}$.

Fig. 15 Arrhenius plot of emission rate constant for trap observed in Au-ZnSe junction.

Table I

Current-Voltage characteristics for Au-ZnSe Schottky Barriers

| Sample | J_0 A/cm ² | Å |
|--------|-------------------------|-----|
| 99 | 1×10^{-10} | 2.0 |
| 100 | 8×10^{-11} | 2.1 |
| 101 | 1×10^{-6} | 4.8 |
| 103 | 3.5×10^{-9} | 2.0 |
| 104 | 1×10^{-6} | 4.8 |

Table II

Au-ZnSe Schottky barrier capacitance voltage characteristics

| Sample | C_o pF | V_{Bi} | $(N_D - N_A) \times 10^{-14} \text{ cm}^{-3}$ |
|--------|----------|----------|---|
| 88 | 40 | 3.5 | 10 |
| 101 | 25 | 1.3 | 2 |
| 103 | 14 | 18 | 8 |
| 104 | 55 | 1 | 10 |
| 105 | 12 | 10 | 8 |

TABLE III

Traps observed in ZnSe/GaAs Heterojunctions

| Trap | Energy eV | Cross section cm ² |
|------|-----------|-------------------------------|
| A | - | - |
| B | .33 | 1×10^{13} |
| C | .35 | 2×10^{-14} |
| D | .54 | 3×10^{-14} |

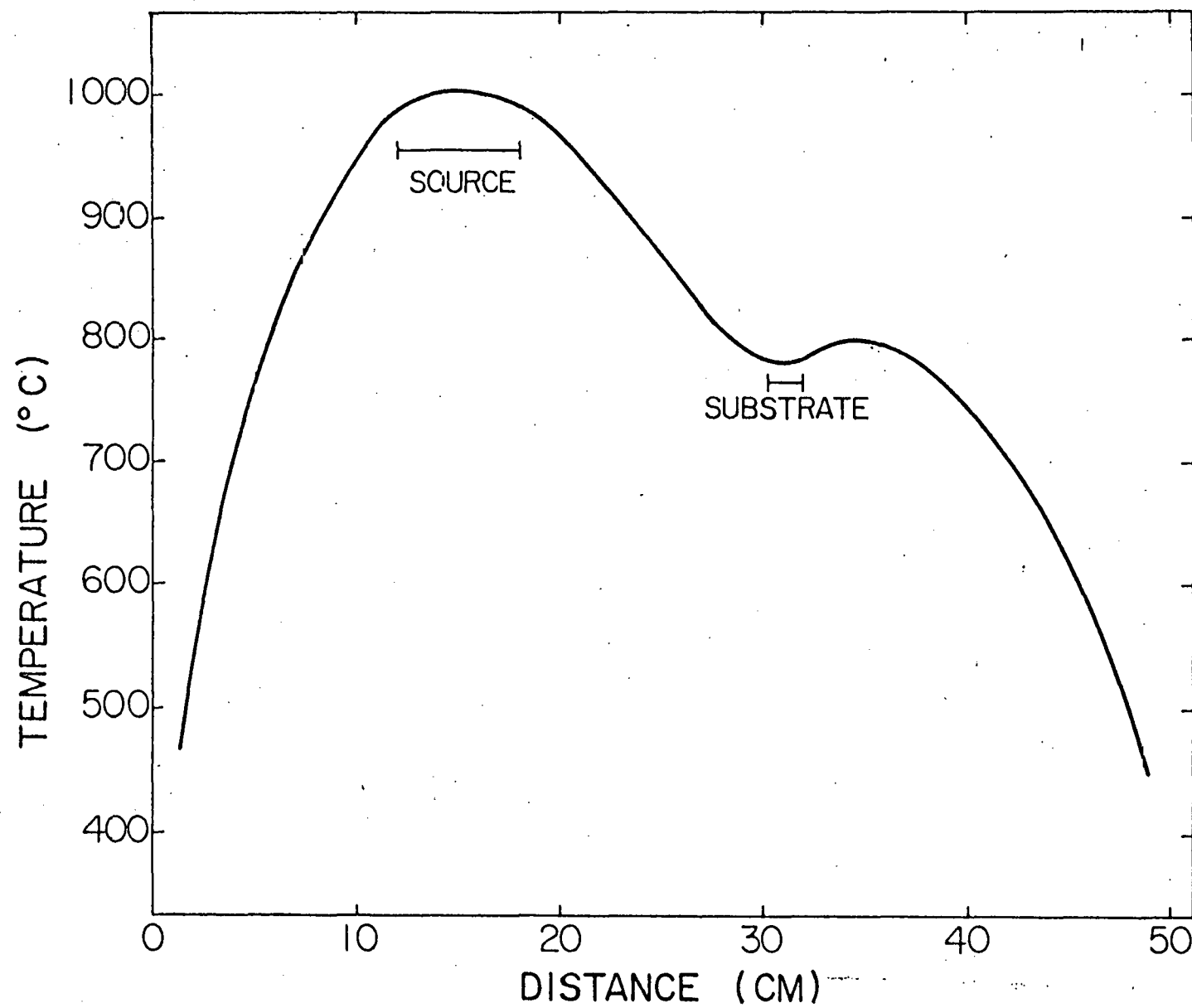


Fig. 1

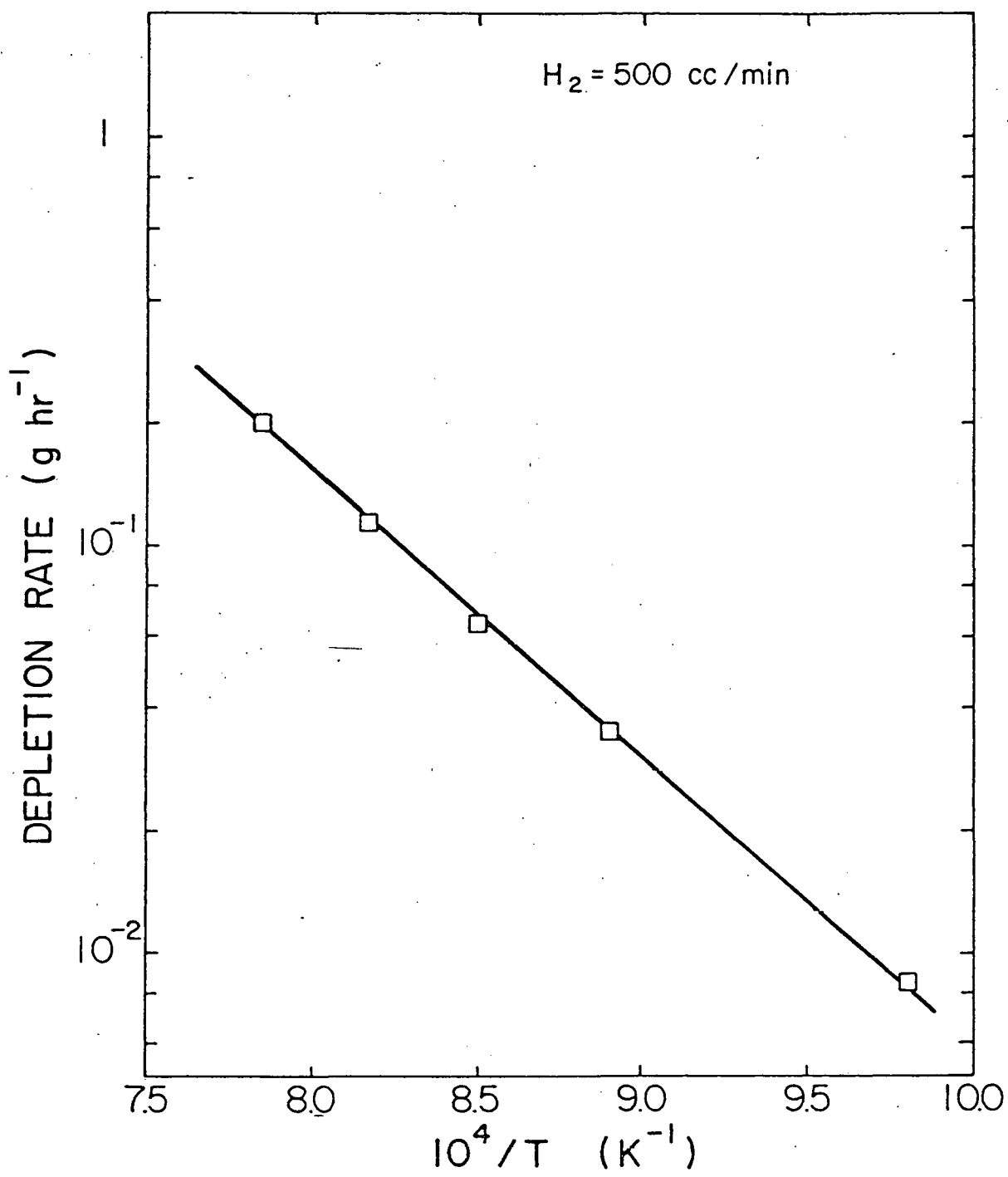


Fig. 2

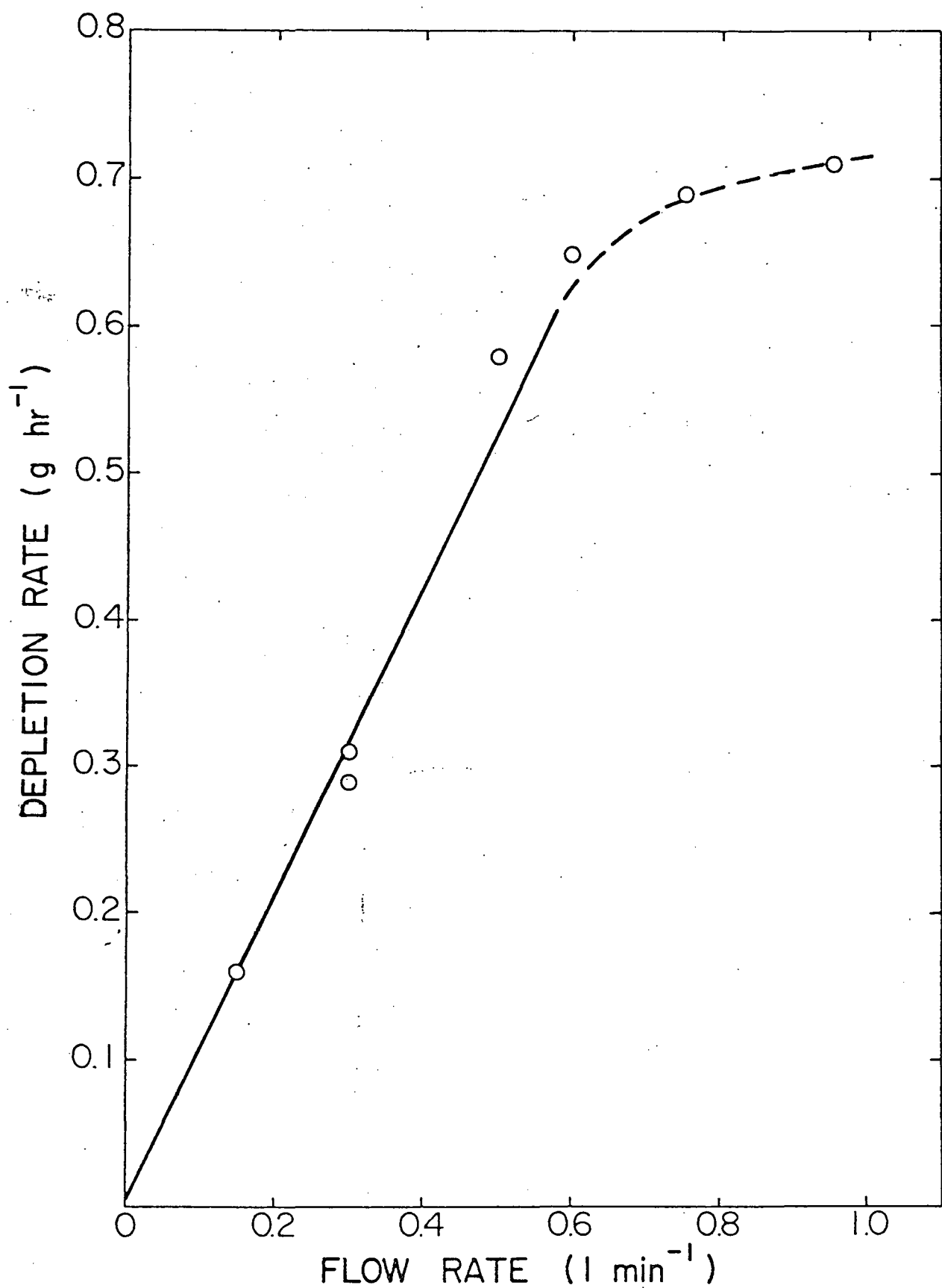


Fig. 3

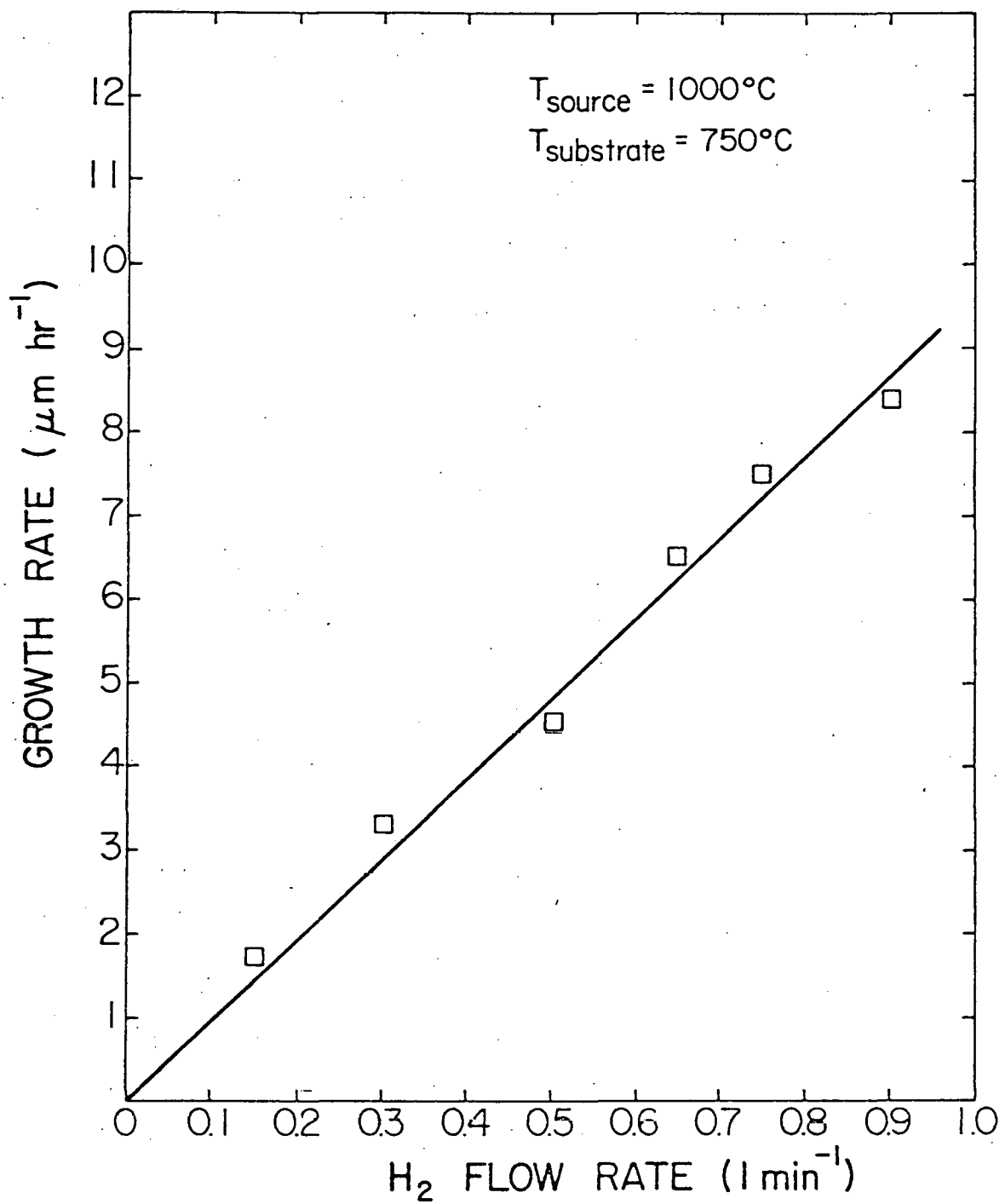


Fig. 4

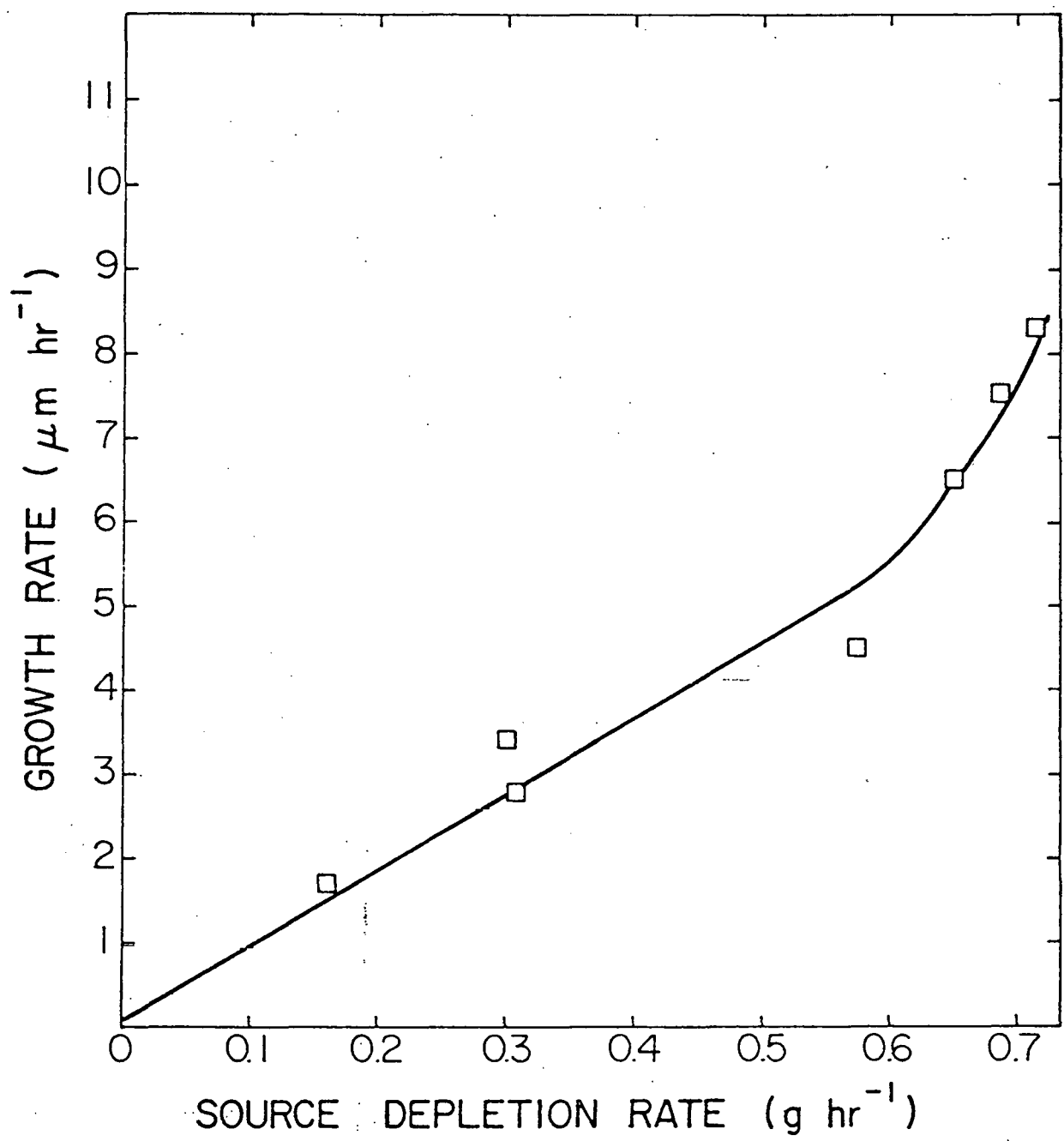


Fig. 5

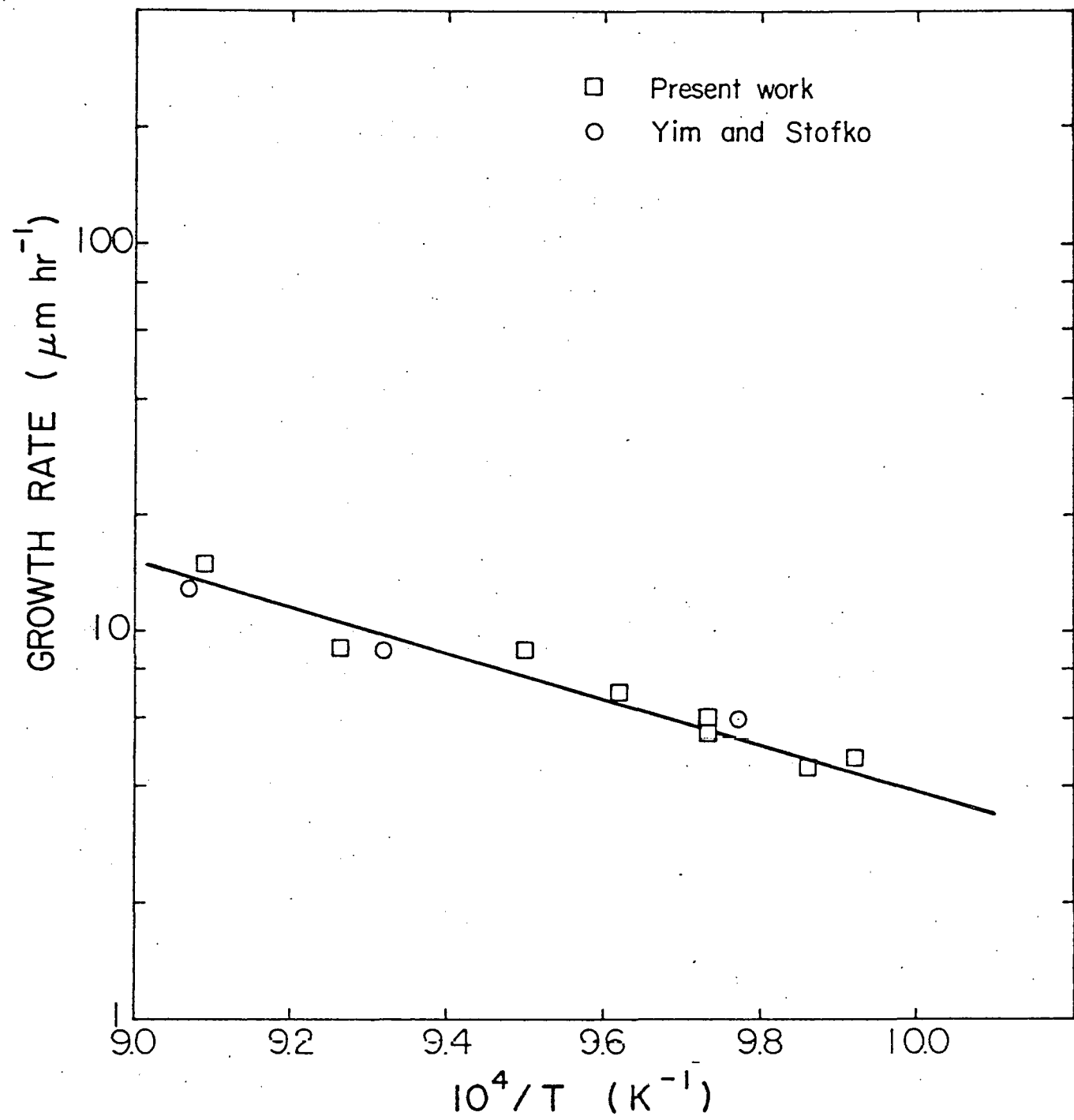


Fig. 6

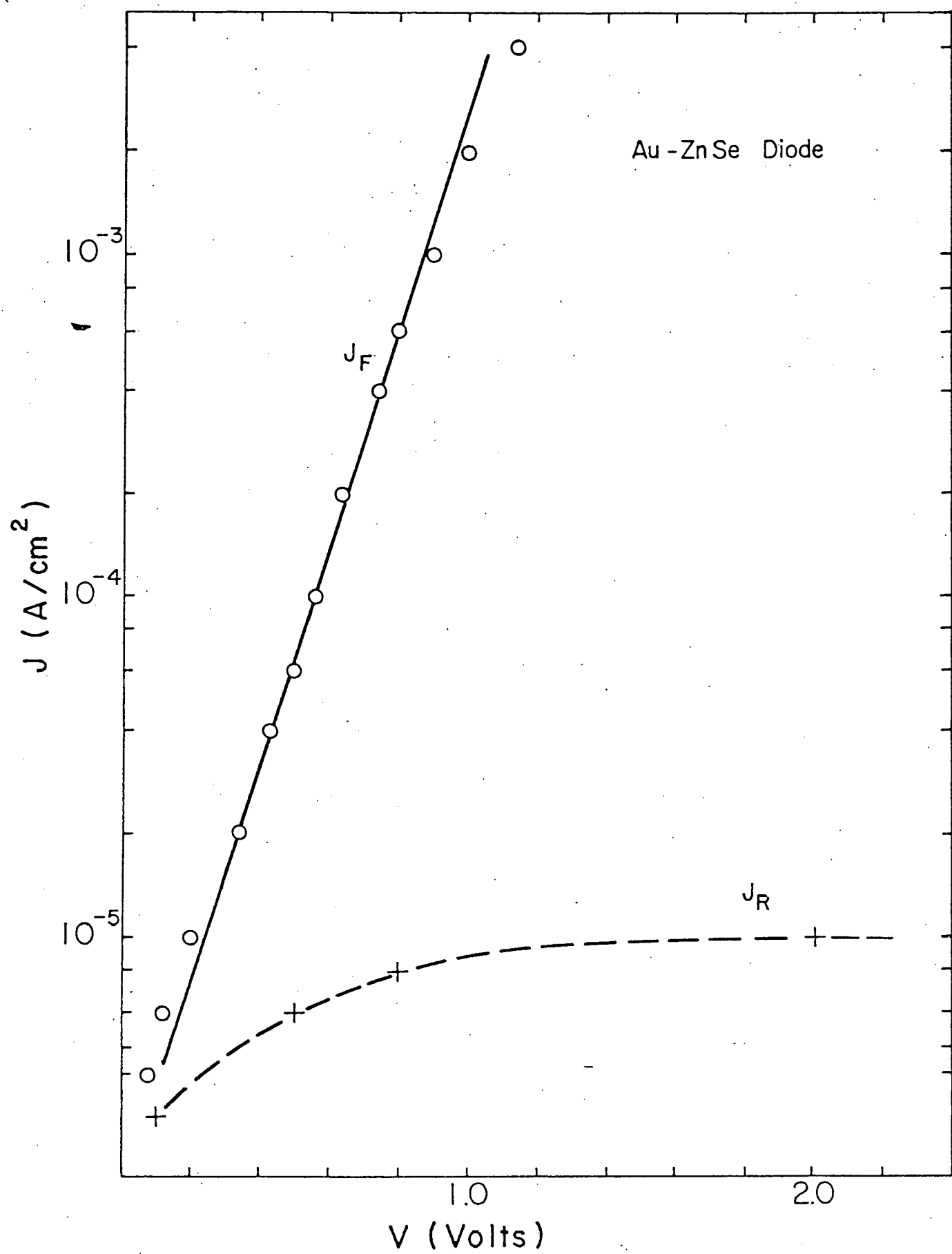


Fig. 7

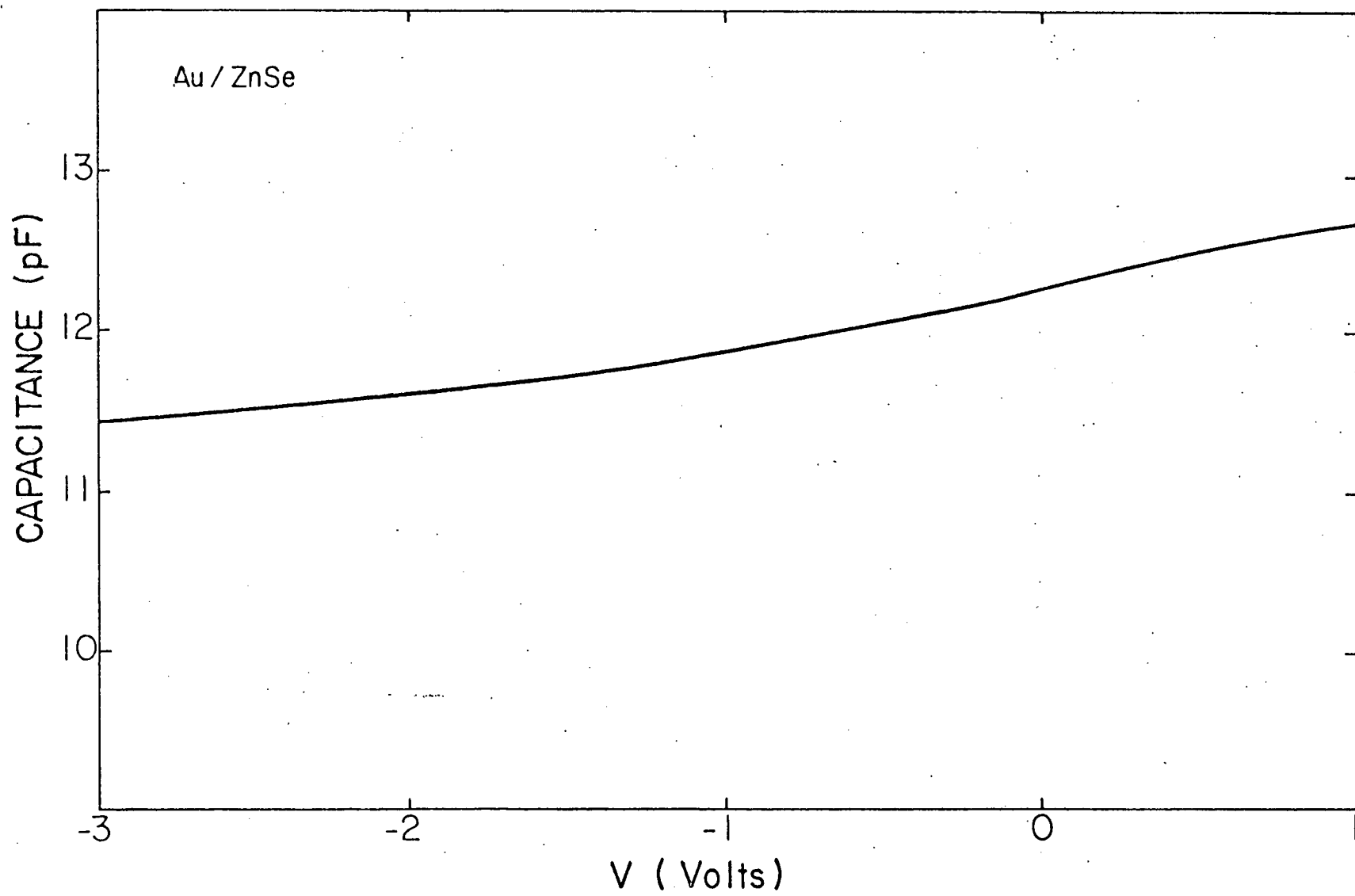


Fig. 8

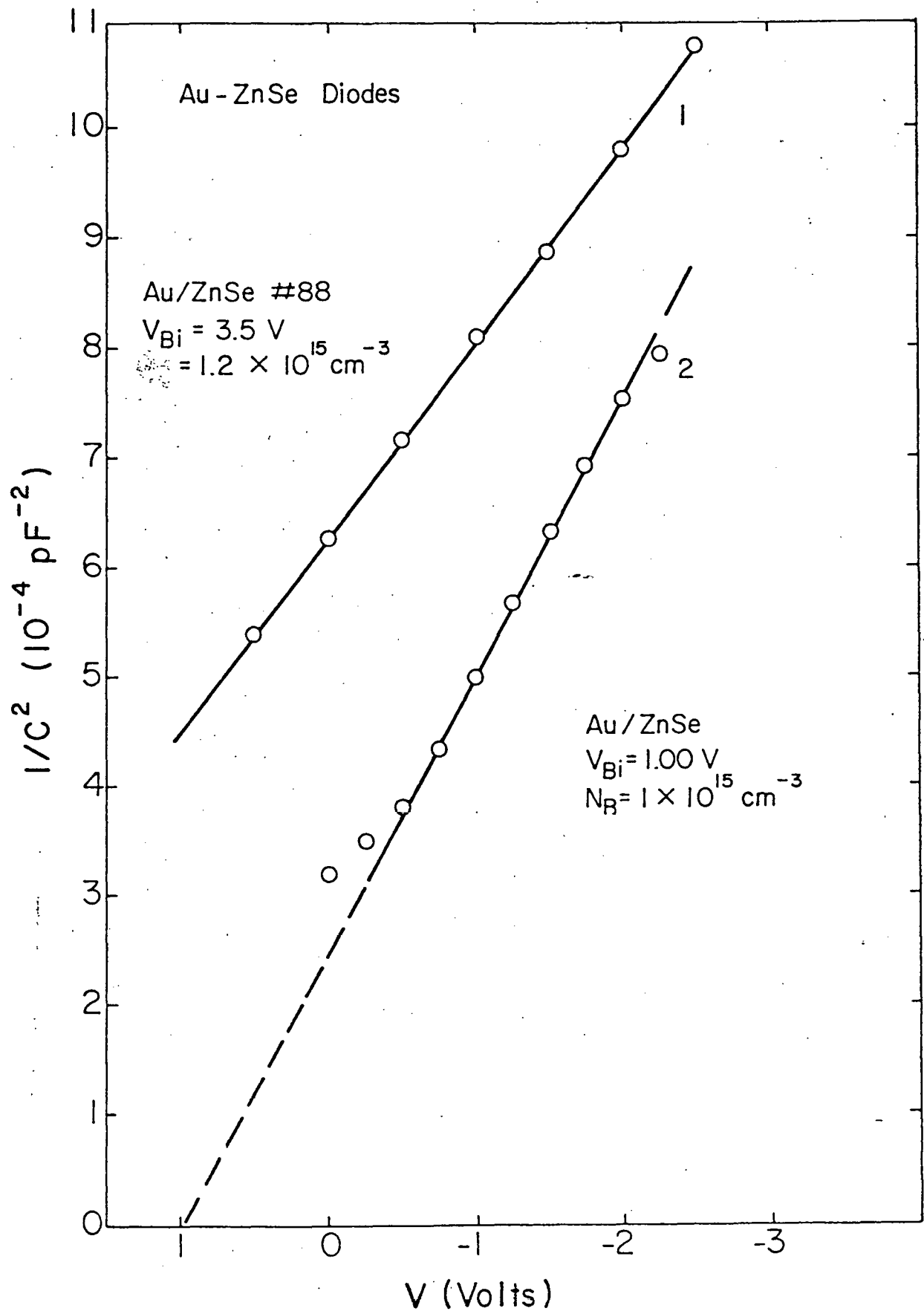


Fig. 9

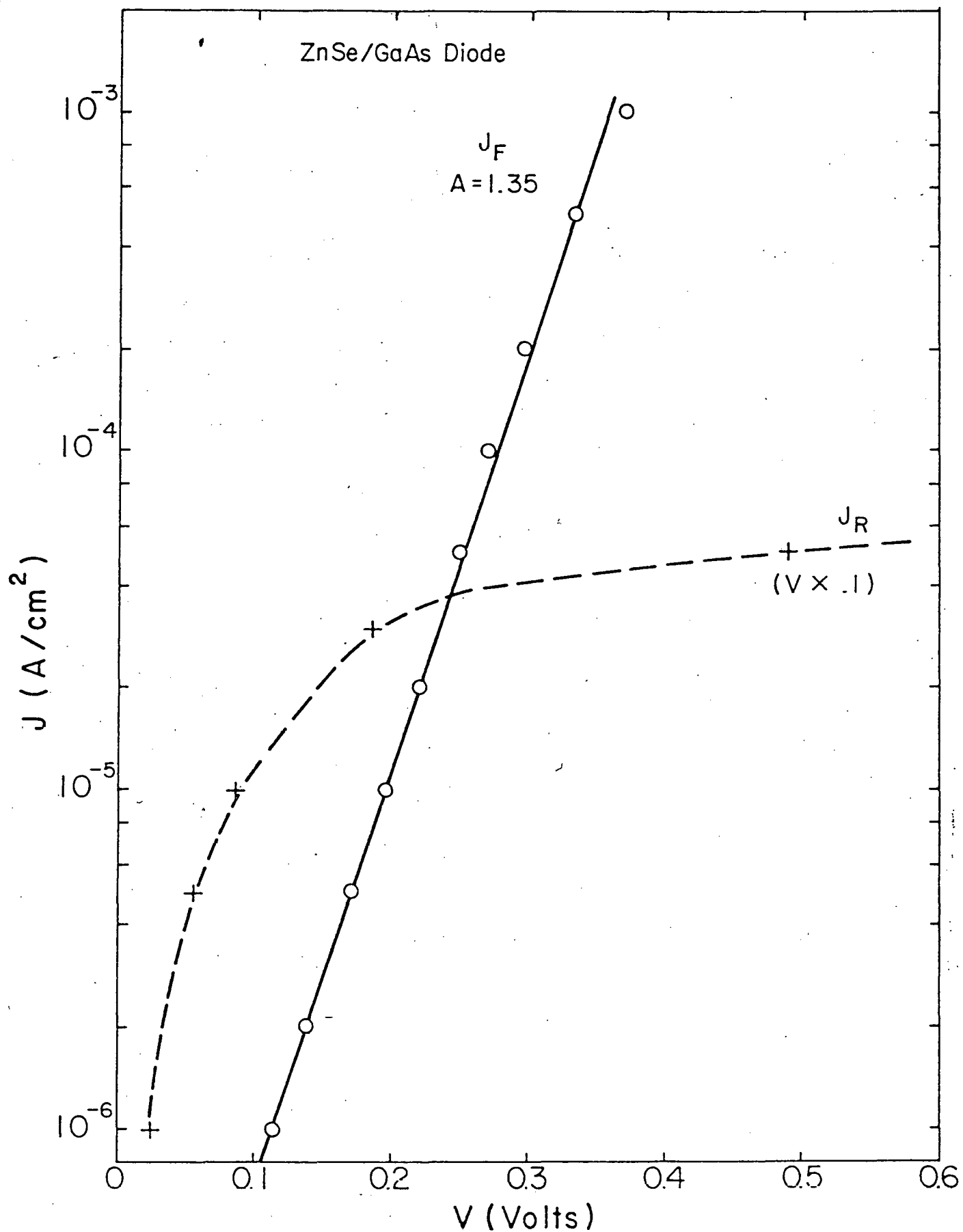


Fig. 10

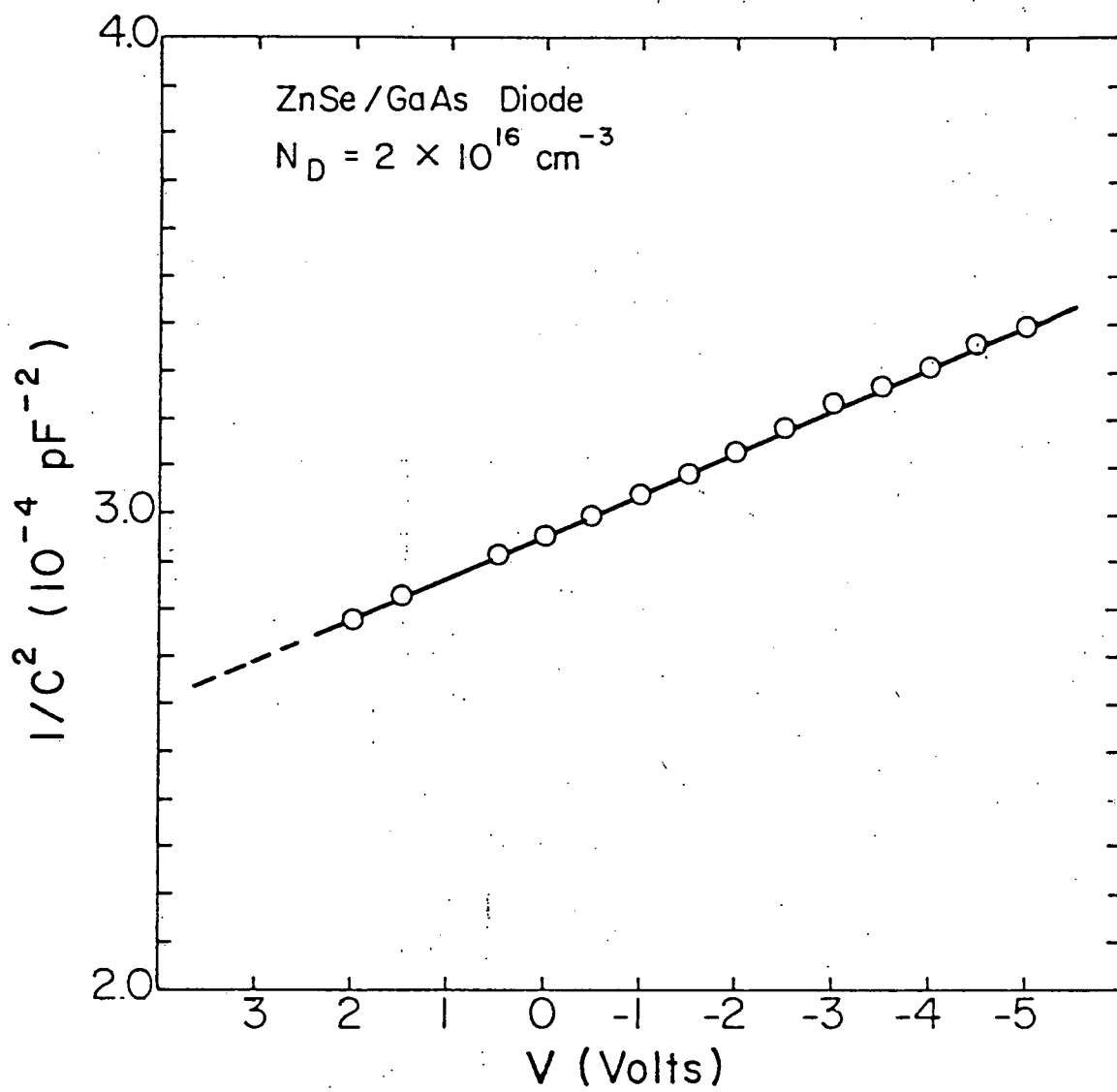


Fig. 11

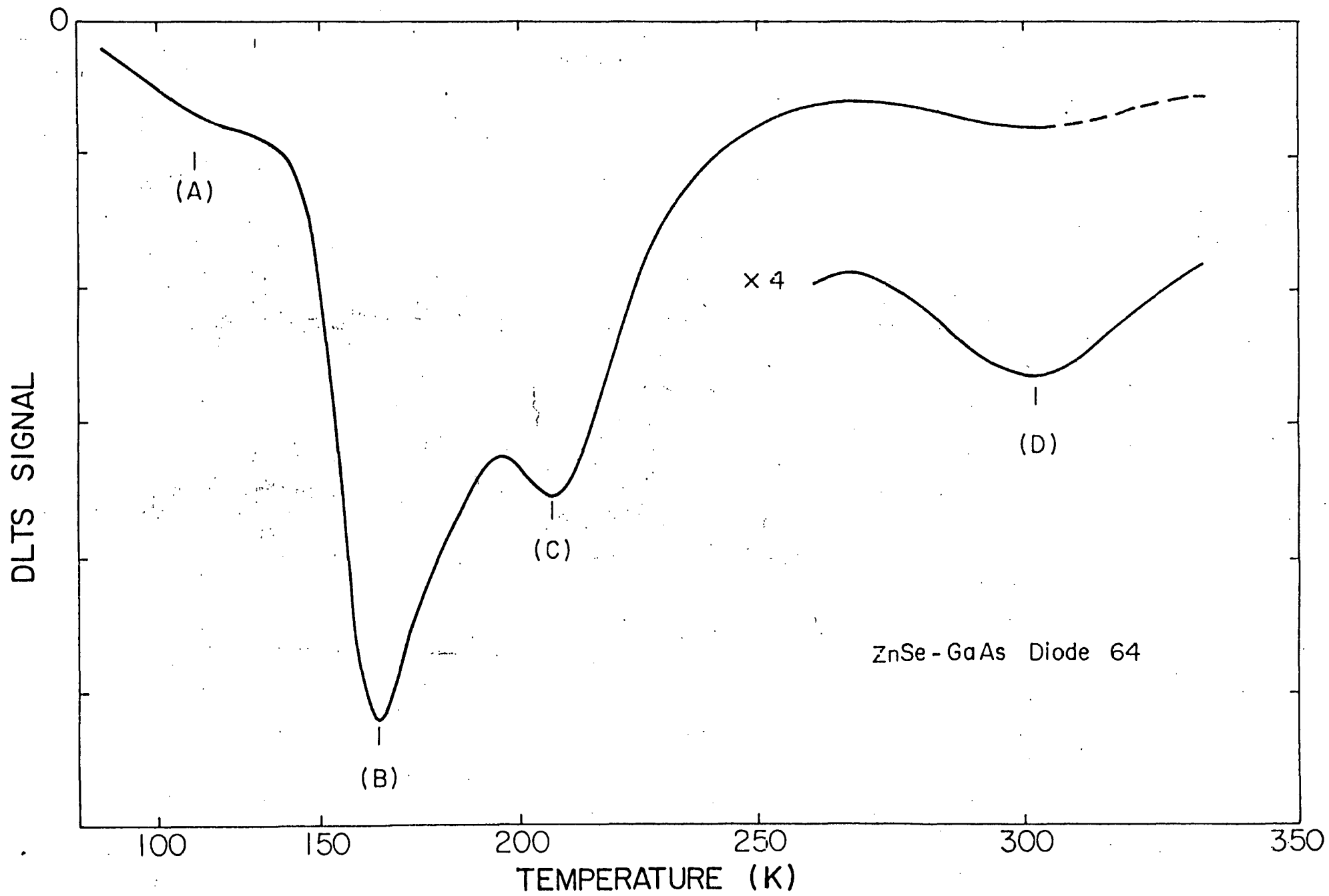


Fig. 12

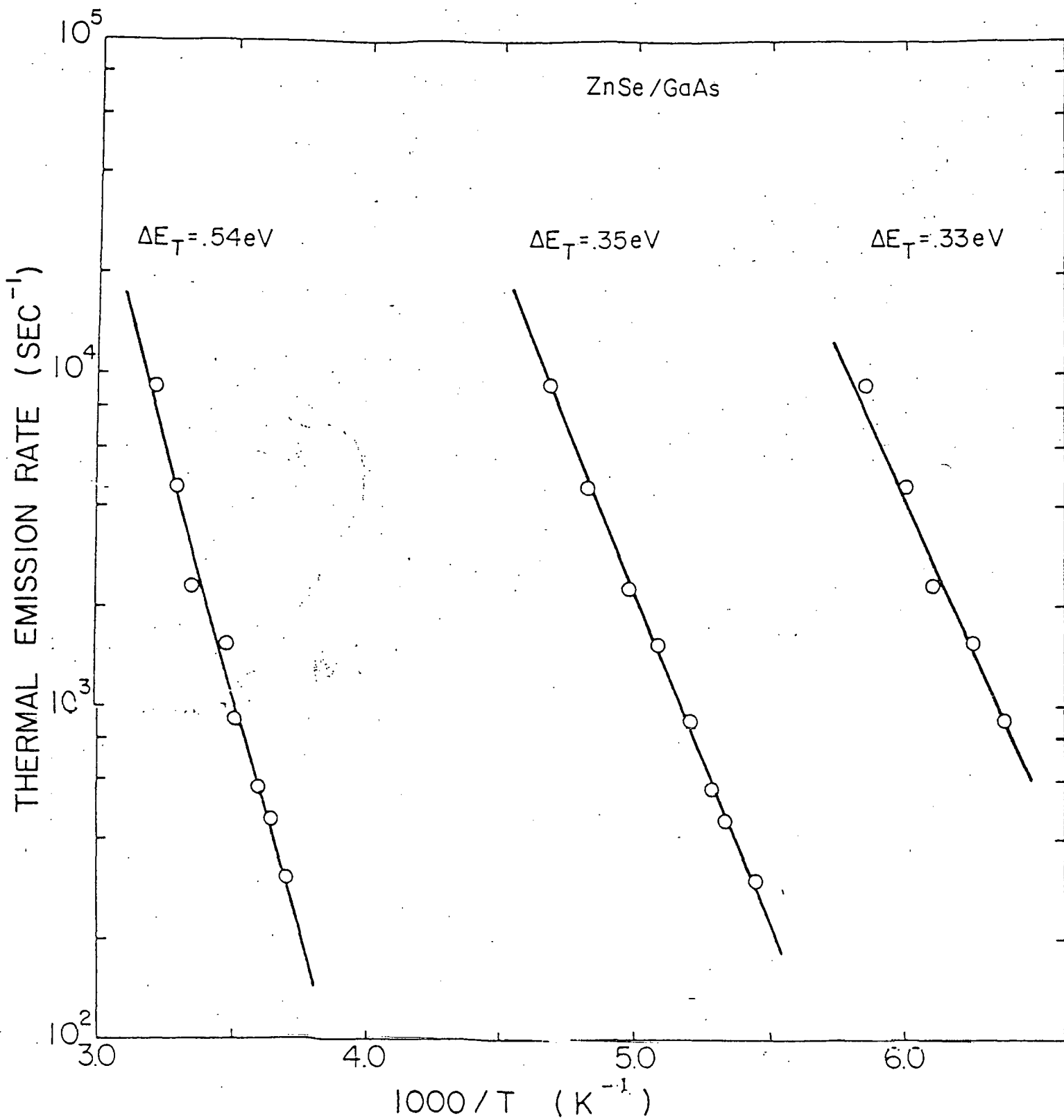


Fig. 13

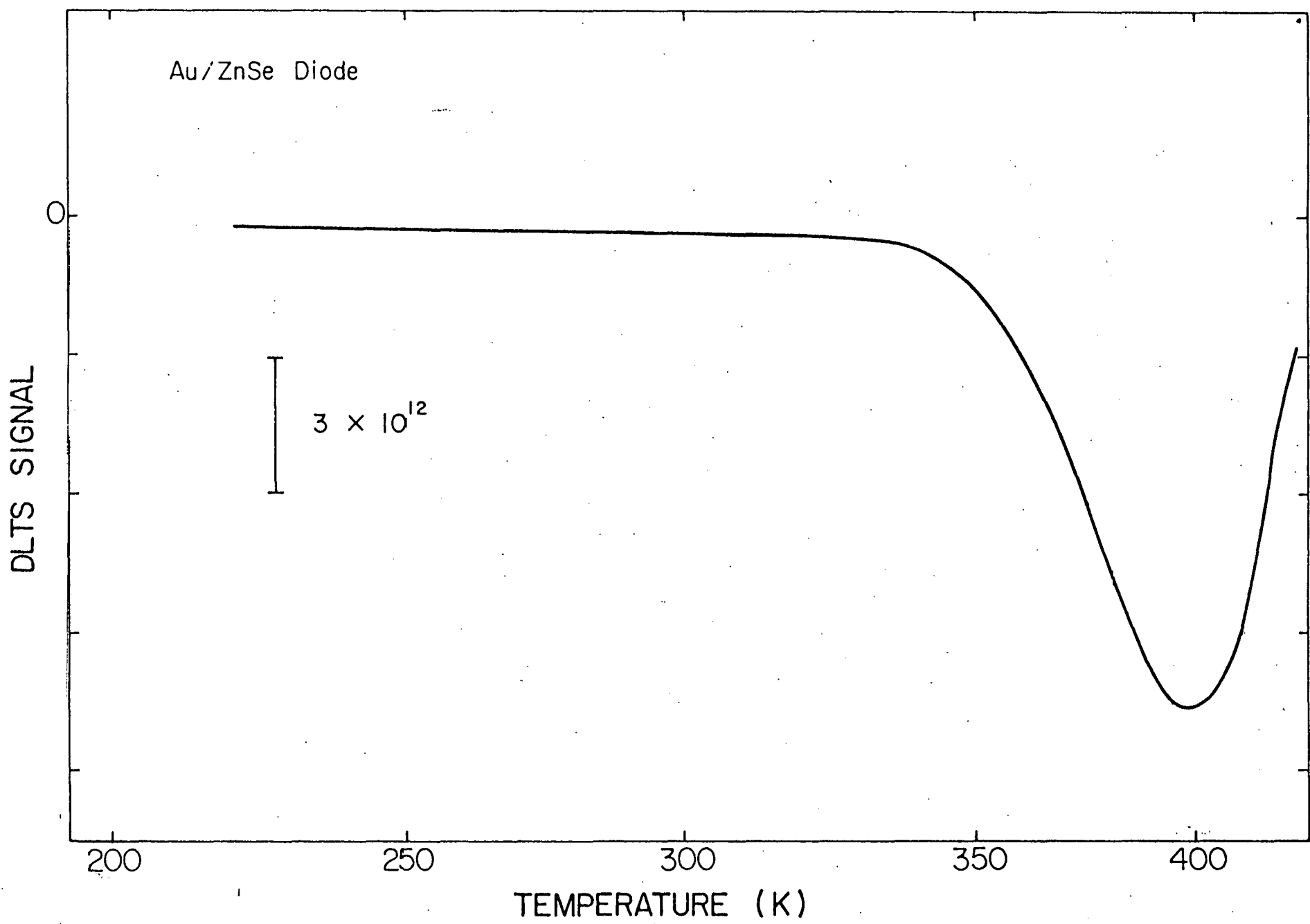


Fig. 14

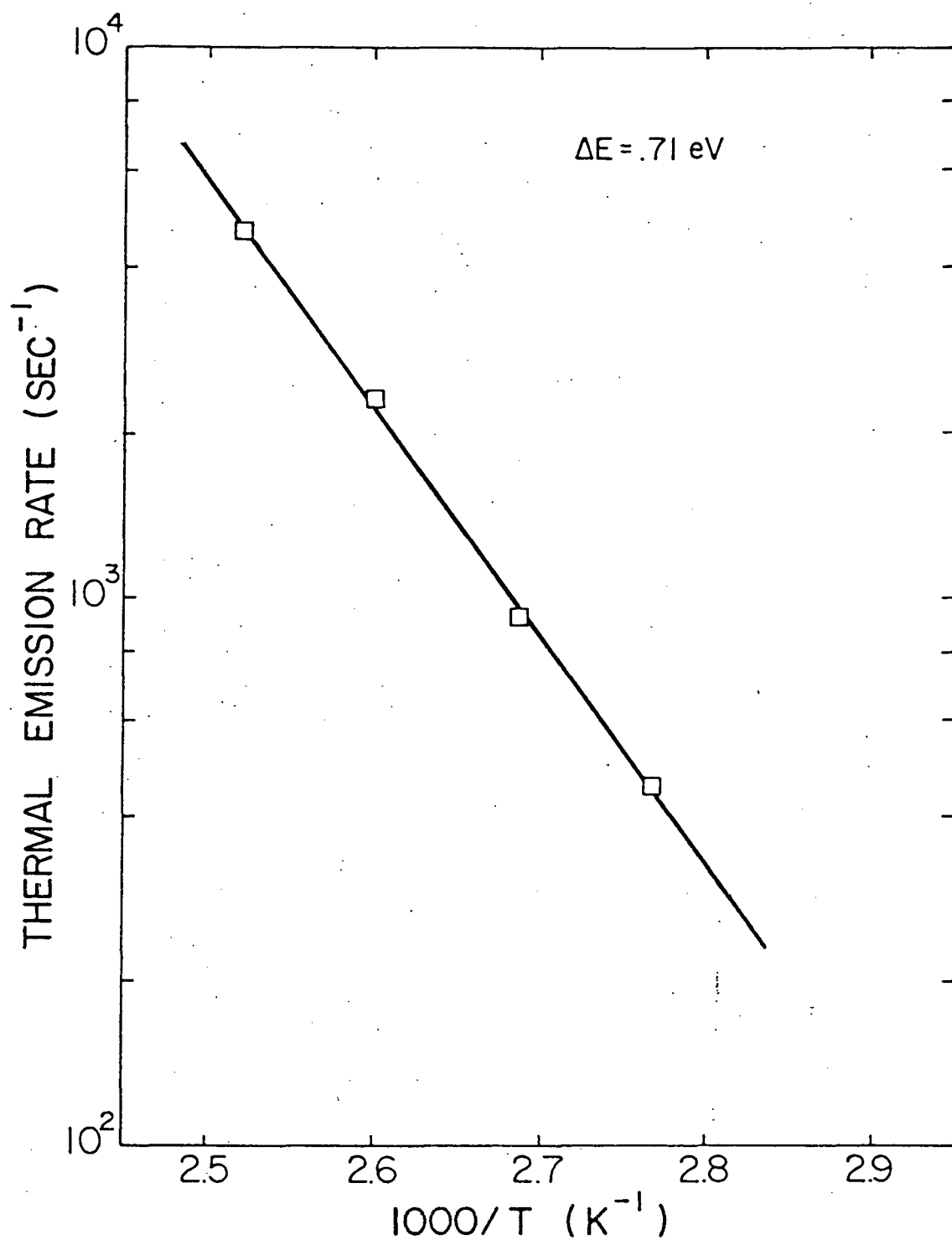


Fig. 15